Materials Science-Poland, Vol. 24, No. 2/2, 2006

Photovoltaic effect in novel polysilane with phenothiazine rings and its blends with fullerene

A. RYBAK[*], J. JUNG, W. CIESIELSKI, J. ULANSKI

Department of Molecular Physics, Technical University of Łódź, 90-924 Łódź, Poland

Investigations of the photogeneration process and photovoltaic effect in recently synthesized polysilane and its mixtures with fullerene (C_{60}) are reported. Dependencies of the photogeneration quantum yield on the wavelength of the exciting radiation and on electric field were determined by the surface potential decay technique. It was found that addition of C_{60} improves the photogeneration efficiency. The Onsager model was used to analyse the obtained results. To check potential application properties of the investigated material, the photovoltaic effect was investigated in devices with an active layer made of mixtures of polysilane and C_{60}. It was found that the power conversion efficiency of the device is dependent on the C_{60} concentration, the photovoltaic effect was observed, however, even if the amount of C_{60} was low (5 wt. %).

Key words: *photovoltaic effect; photogeneration quantum yield; polysilane; fullerene*

1. Introduction

Silicon-backbone oligomers and polymers – polysilanes – are functional polymer materials exhibiting interesting photophysical properties. Polysilanes are also attractive photoconductive materials due to a relatively high mobility of charge carriers. A substitution of side groups by chromophores and doping are required, however, in order to enhance their sensitivity in the visible range [1–6]. For this reason, a novel polysilane copolymer was synthesised, with *N*-phenothiazine moiety attached to the main chain with an *n*-propyl spacer (hereafter referred to as PSi–Phth, see Fig. 1) was synthesised. The main purpose for introducing the phenothiazine side groups was to facilitate the ability of C_{60} fullerene to be attached to the polysilane chain, and therefore to create a donor–acceptor system. Because of a non-planar structure of phenothiazine, the fullerene molecule is better connected. The mixture PSi–Phth/C_{60} was used as active layer in photovoltaic cells. It is well known that addition of fullerene

---

[*] Corresponding author, e-mail: Andrzej.Rybak@p.lodz.pl

(which is a strong electron acceptor) to semiconducting polymers increases the photoconductivity [7–9].

Fundamental processes in photoconduction and photovoltaic effect are: photogeneration of charge carrier pairs, their separation and then transport of electrons and holes. Preparation of a suitable donor and acceptor mixture can organize the molecules into phase-separated, interpenetrating and continuous donor and acceptor network. The large effective interface can be reached by photo-excitons and increases probability of the charge carriers photogeneration. One can use such a mixture for fabricating efficient photovoltaic devices [10–15].

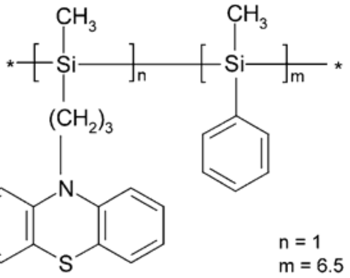

Fig. 1. Molecular structure of PSi–Phth copolymer

Dependencies of the photogeneration quantum yield on photon flux, on light wavelength and on electric field in the copolymer/fullerene mixtures were determined using the surface potential discharge (SPD) technique [15–17]. The influence of fullerene addition on the performance of the photovoltaic devices was also investigated.

2. Experimental

Materials. Newly synthesized *N*-phenothiazine-substituted polysilane: poly[[3-(N -phenothiazinyl)propyl]methylsilane-co-methylphenylsilane] containing phenothiazine moieties connected to the main polysilane chain *via* a short *n*-propyl spacer (Fig. 1) was investigated. The copolymer was synthesized by the Wurtz coupling reaction of corresponding monomers, ie. [3-(N-phenothiazinyl)propyl]methyldichlorosilane and dichloromethylphenylsilane. All reagents and starting materials were purchased from Sigma -Aldrich and were used without further purification. C_{60} was used as electron acceptor and electron transport material in the blend devices. UV-Vis absorption spectra of the investigated materials and of their blend are shown in Figure 2. The spectra of the individual components are additive, i.e., the spectrum of a mixture is a weighted sum of the spectra of pure components. This feature means that no distinct charge transfer (CT) band was detected.

Preparation of samples for surface potential decay technique and evaluation of the photogeneration quantum yield. Samples for the SPD measurements were prepared on stainless steel substrates by drop casting from toluene solution (20 mg/ml) of pure

PSi–Phth and its mixture with 5 wt. % of C_{60}. A slow, limited evaporation rate yields homogeneous films of 2 μm in thickness. The thicknesses of the investigated samples were determined with an AFM microscope (NT-MDT Solver Pro).

The SPD technique is described in details elsewhere [15–17]. Briefly, it consists in charging the sample surface in the dark to an initial potential V_S by the corona discharge (the ions form a blocking electrode on the sample surface) and monitoring the surface potential decay, first in the dark, and then under illumination with a selected wavelength. Because the concentration of trapped charge carriers and recombination centres increases during the steady-state illumination, and it is difficult to take these processes into consideration, only the initial photo-induced discharge is analysed, i.e. the surface potential derivative at the moment t_0 (start of the illumination) is determined and used for further analysis [16].

For the emission-limited discharge, the photogeneration quantum yield ϕ is given by the equation [17]:

$$\phi = \frac{\varepsilon\varepsilon_0 S}{e n_{\mathrm{ph}} d}\left(\frac{dV}{dt}\right)_{t_0} \tag{1}$$

where: ε is the relative electric permittivity of the material; ε_0 – permittivity of free space, S – the surface area, e – the unit charge, n_{ph} – the number of the absorbed photons per unit time, d – the thickness of the sample, (dV/dt) is the rate of decay of the surface potential; t_0 indicates the initial moment of the irradiation of the sample.

The SPD measurements were performed with the continuous monochromatic incident radiation. A PTI power arc mercury-xenon lamp with various band-pass and grey filters was used as a light source. To check if the emission-limited condition is fulfilled, the discharge measurements were performed with different photon flux densities n_{ph} in the range 10^{16}–10^{19} photons/($\mathrm{m}^2 \cdot \mathrm{s}$). The quantum yield was calculated from the measured photodecays taking into account corrections for the light source performance, spectral characteristic of the optical path and absorption by the active area of the sample. All the measurements were carried out at room temperature under ambient conditions.

Preparation of the photovoltaic devices and the photovoltaic effect measurements. The photovoltaic effect was measured on samples prepared in ambient conditions by spin casting toluene solutions of the investigated material (20 mg/ml) onto indium –tin–oxide (ITO) coated glass substrates at room temperature. The ITO electrode had been earlier covered with a 20 nm film of poly(ethylenedioxythiophene) doped with polystyrene sulfonic acid (PEDOT-PSS). Different concentrations (0–80 wt. %) of fullerene in the mixture with PSi–Phth were used. On top of the film, a 150 nm thick aluminium electrode was evaporated.

The devices were illuminated through the ITO electrode with light whose intensity amounted 1 mW/cm^2 using a xenon lamp with monochromatic filters (at $\lambda = 340$, 405, 500 nm). Current–voltage characteristics were measured in air using a computer controlled source-measure unit (Keithley 2410). The power conversion efficiency η was calculated as the ratio of the maximal electrical power generated in the cell ($P_{\max}$) to the power of incident light (P_{in}):

$$\eta = \frac{P_{\max}}{P_{\mathrm{in}}} = FF\frac{U_{\mathrm{OC}}J_{\mathrm{SC}}}{LA} \tag{2}$$

where A is equal to the illuminated surface area (ca. 0.06 cm^2), L is the intensity of the incident light (not corrected for absorption-reflection processes at the ITO-covered surface), and FF is the fill factor ($FF = (UI)_{\max} / (U_{\mathrm{OC}}I_{\mathrm{SC}})$), U_{OC} being the open circuit voltage, and I_{SC} – the short circuit current.

3. Results and discussion

3.1. Photogeneration in PSi–Phth and its mixture with C_{60}

Figure 2 shows spectral dependencies of the photogeneration quantum yield ϕ for the PSi–Phth and PSi–Phth/C_{60} samples, and their UV-Vis absorption spectra for the whole investigated wavelength range, from 270 nm to 680 nm. One can observe a coincidence of the maximum of ϕ with the optical absorption maximum at *ca* 340 nm. The photogeneration efficiency decreases at the long wavelength absorption tail. This symbatic dependence indicates that there is no photoinjection of charge carriers from the substrate electrode by the weakly absorbed light.

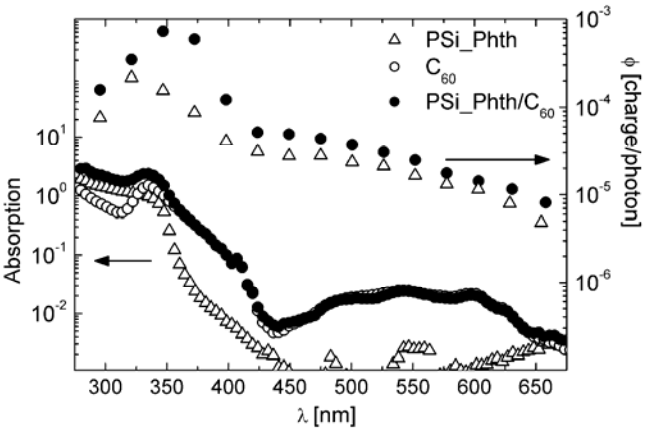

Fig. 2. UV-Vis absorption spectra (left axis) for PSi–Phth ($n = 1$, $m = 6.5$) copolymer, fullerene and their mixture (5 wt. % of C_{60}) in solutions in toluene and spectral dependencies of the photogeneration quantum yield ϕ (right axis) measured for PSi–Phth and for PSi–Phth/C_{60} blend layers obtained by drop casting; $E = 1.2\times10^8$ V/m, $n_{\mathrm{ph}} = 10^{19}$ photons/m^{2}s, $d = 2$ μm, $S = 3.14\times10^{-4}$ m^2, $\varepsilon = 3$ was taken for the calculations

Photogeneration in the PSi–Phth layer is enhanced in the spectral range between 320 nm and 430 nm by doping with C_{60}, as is shown in Figure 2. As no CT band was detected in the absorption spectrum of the blend, the improvement of photogeneration should therefore be due to a superposition of photogeneration processes of individual components. The increase of the photogeneration efficiency in the steady state photoconductivity measurements in fullerene samples was described in terms of the intermolecular charge transfer states within the fullerene aggregates [18–21]. Figure 3 presents the electric-field dependencies of ϕ in PSi–Phth (a) and in its mixture with 5 wt. % of C_{60} (b).

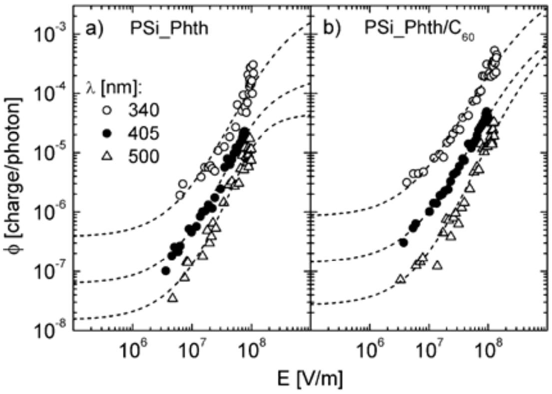

Fig. 3. The electric-field dependence of the photogeneration quantum yield ϕ for various wavelengths in: a) the pure PSi–Phth layer, b) for PSi–Phth + 5 wt. % C_{60} layer. The photon flux $n_{ph} = 10^{19}$ photons/m^{2}s, the samples thickness $d = 2$ μm. The dashed lines were obtained by fitting the experimental data with the Onsager model assuming a delta distribution of the thermalization length r_0 and $\varepsilon = 3$

The field dependencies of the photogeneration quantum yield in both samples can be well described by the model based on the Onsager theory of geminate recombination [22, 23]. One can get the primary photogeneration quantum yield ϕ_0 and the thermalization length r_0 by fitting the experimental data. The values of ϕ_0 and r_0 were obtained assuming a delta distribution of r_0. One should nevertheless note that a limited range of electric fields available in the SPD experiment does not allow us to exclude other distributions. It was shown that when a CT complex is involved in the photogeneration, the data cannot be fitted by the Onsager model and the kinetic model proposed by Braun is more suitable [24, 25]. A good matching with the Onsager model points to the absence of a CT complex in the PSi–Phth/C_{60} mixtures. The fitting parameters are collected in Table 1. One can see that for all the investigated wavelengths of exciting light r_0 is almost constant, while ϕ_0 considerably decreases at longer wavelengths. It is interesting to note that the thermalization length r_0 in PSi–Phth/C_{60} is comparable with the diameter of C_{60} molecule (0.7 nm).

On comparing ϕ values obtained for the PSi–Phth and PSi–Phth/C_{60} samples at the same electric field one finds that the photogeneration quantum yield is higher for the system with C_{60} and this effect is stronger at low electric fields (Fig. 3).

Table 1. Primary photogeneration quantum yield ϕ_0 and thermalization length r_0 in PSi–Phth copolymer (pure and with 5 wt. % of C_{60}, for various excitation wavelengths) calculated using the Onsager theory of geminate recombination with assumed delta distribution of r_0

Copolymer	λ [nm]	340	405	500
PSi–Phth	ϕ_0	3.5×10^{-3}	2.5×10^{-4}	4.7×10^{-5}
	r_0 [nm]	2.3	2.9	2.8
PSi–Phth + 5 wt. % C_{60}	ϕ_0	1.6×10^{-2}	4.7×10^{-3}	5.5×10^{-3}
	r_0 [nm]	0.6	0.5	0.4

3.2. Photovoltaic effect in PSi–Phth/C_{60}

Figure 4 shows *I–U* characteristics obtained for different wavelengths of exciting light in a device with PSi–Phth containing 50 wt. % of C_{60}. The determined values of short circuit current density (J_{SC}), open circuit voltage (U_{OC}), fill factor (*FF*), and power conversion efficiency (η) are listed in Table 2. The best photovoltaic parameters are achieved for the illumination with $\lambda = 405$ nm. This result is inconsistent with the spectral dependence of the photogeneration quantum yield ϕ, indicating that it is not only photogeneration that contributes to the generation of charges but also photoinjection from the illuminated organic material-metal electrode junction plays a significant role.

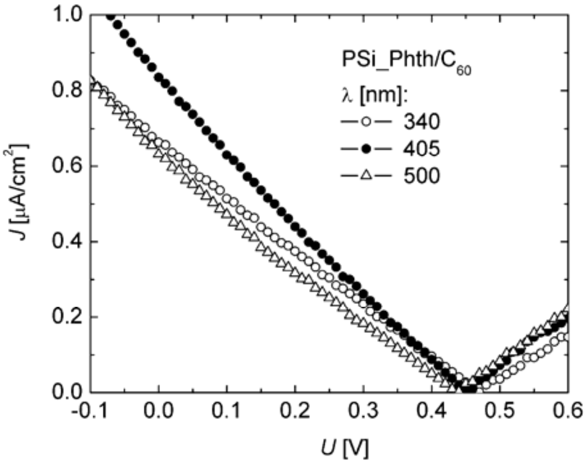

Fig. 4. *I–U* characteristics of the photovoltaic devices made of PSi–Phth + 50 wt. % C_{60} for various wavelengths. Active area was *ca.* 0.06 cm^2, thickness $d = 140$ nm, and the light intensity $L \approx 1.0$ mW/cm^2

Figure 5 shows *I–U* characteristics obtained for various mass fractions of fullerene in PSi–Phth/C_{60} devices illuminated with $\lambda = 405$ nm. It is clearly seen that there is no photovoltaic effect in pure PSi–Phth, while the performance of the device improves

Table 2. The short circuit current J_{SC}, open circuit voltage U_{OC}, fill factor *FF*, the energy conversion efficiency η for various wavelengths λ in PSi–Phth + 50 wt. % C_{60} photovoltaic devices

λ [nm]	J_{SC} [µA/cm^2]	V_{OC} [V]	FF [%]	η [%]
340	0.66	0.48	24.0	0.0064
405	0.84	0.45	23.7	0.0128
500	0.63	0.44	23.6	0.0066

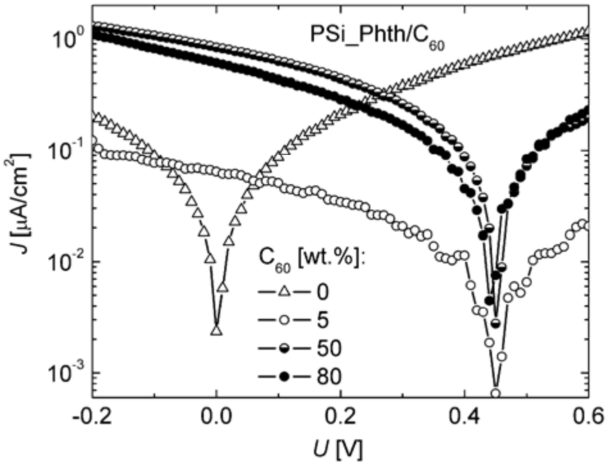

Fig. 5. *I–U* characteristics of the photovoltaic devices with various contents of fullerene. Active area *ca.* 0.06 cm^2, thickness d = 140 nm, excitation at λ = 405 nm, light intensity L = 0.7 mW/cm^2

with increased fullerene fraction. Because photogeneration occurs both in pure PSi –Phth and in PSi–Phth/C_{60} (Figs. 2 and 3), this effect demonstrates that fullerene improves the transport of photogenerated electrons to the anode (holes are transported by polysilane chain to the cathode). However, as is shown in Fig. 5, the amount of the fullerene should not be too high: the performance of the PSi–Phth/C_{60} device with 80 wt. % of C_{60} is worse than that is the system with 50 wt. % of C_{60}, probably due to a worse connectivity of the polymer network.

4. Conclusions

The photogeneration quantum yield in polysilane copolymer with phenothiazine side groups increases upon addition of fullerene acceptor, although no CT complex is formed and the photogeneration mechanism can be described by the Onsager model. The decrease of r_0 with increasing amount of fullerene indicates that in PSi–Phth/C_{60} mixtures the photogeneration proceeds rather within the fullerene aggregates than in polysilane copolymer.

The photovoltaic effect appears after introducing even small amounts of C_{60} to the polysilane copolymer with phenothiazine moieties. One can conclude that the presence of C_{60} facilitates the separation of the photogenerated electron/hole pairs and also creates transport channels for electrons.

Acknowledgements

This work was supported by the NAIMO Integrated Project No NMP4-CT-2004-500355.

References

[1] NESPUREK S., SWORAKOWSKI J., Thin Solid Films, 396 (2001), 168.
[2] NESPUREK S., TOMAN P., SWORAKOWSKI J., LIPINSKI J., Curr. Appl. Phys., 2 (2002), 299.
[3] NESPUREK S., Czech. J. Phys., 49 (1999), 859.
[4] NESPUREK S., PFLEGER J., BRYNDA E., KMINEK I., KADASHCHUK A., VAKHNIN A., SWORAKOWSKI J., Mol. Cryst. Liq. Cryst., 355 (2001), 191.
[5] CIMROVA V., KMINEK I., NESPUREK S., SCHNABEL W., Synth. Met., 64 (1994), 271.
[6] GLOWACKI I., JUNG J., ULANSKI J., Synth. Met. 109 (2000), 143.
[7] WANG Y., Nature, 356 (1992), 585.
[8] SARICIFTCI N.S., SMILOWITZ L., HEEGER A.J., WUDL F., Science, 258 (1992), 1474.
[9] HALLS J.J.M., PICHLER K., FRIEND R.H., HOLMES S.C., MORATTI A.B., Synth. Met., 77 (1996), 277.
[10] SCHMIDT-MENDE L., FECHTENKÖTTER A., MÜLLEN K., MOONS E., FRIEND R.H., MACKENZIE J.D., Science, 293 (2001), 1119.
[11] DYAKONOV V., Physica E, 14, 53 (2002).
[12] NEUGEBAUER H., BRABEC C., HUMMELEN J.C., SARICIFTCI N.S., Sol. Ener. Mater. Sol. Cells, 61 (2000), 35.
[13] PADINGER F., RITTBERGER R.S., SARICIFTCI N.S., Adv. Funct. Mater., 11 (2003), 1.
[14] KATZ E.A., Phys. Solid State, 44 (2002), 621.
[15] JUNG J., RYBAK A., SLAZAK A., BIALECKI S., MISKIEWICZ P., GLOWACKI I., ULANSKI J., ROSSELLI S., YASUDA A., NELLES G., TOMOVIĆ Z., WATSON M.D., MÜLLEN K., Synth. Met., 155 (2005), 150.
[16] BORSENBERGER P.M., WEISS D.S., *Organic Photoreceptors for Imaging Systems*, Marcel Dekker, New York, 1993, p. 276.
[17] BERG W.F., HAUFFE K. (Eds.), *Current Problems in Electrophotography*, Walter de Gruyter, Berlin, 1972, p. 225.
[18] GIRO G., KALINOWSKI J., DIMARCO P., FOTTORI V., MARCONI G., Chem. Phys. Lett., 211 (1993), 580.
[19] KAZAOUI S., ROSS R., MINAMI N., Phys. Rev. B, 52 (1995), R11665.
[20] KAZAOUI S., ROSS R., MINAMI N., Synth. Met., 70 (1995), 1403.
[21] KOCHER M., DAUBLER T.K., HARTH E., SCHERF U., GUGEL A., NEHER D., Appl. Phys. Lett., 72 (1998), 650.
[22] ONSAGER L., Phys. Rev., 54 (1938), 554.
[23] MOZUMDER A., J. Chem. Phys., 60 (1974), 4300.
[24] BRAUN C.L., J. Chem. Phys., 80 (1984), 4157.
[25] JUNG J., GLOWACKI I., ULANSKI J., J. Chem. Phys., 110 (1999), 7000.

Received 15 October 2005
Revised 25 November 2006